British Journal of Pharmacology

DOI:10.1111/j.1476-5381.2011.01359.x
www.brjpharmacol.org

RESEARCH PAPER

Generation and characterization of a humanized PPARδ mouse model

B Gross[1,2,3,4], N Hennuyer[1,2,3,4], E Bouchaert[1,2,3,4], C Rommens[1,2,3,4], D Grillot[5], H Mezdour[4] and B Staels[1,2,3,4]

[1]*Université Lille Nord de France, Lille, France,* [2]*Inserm, U1011, Lille, France,* [3]*UDSL, Lille, France,* [4]*Institut Pasteur de Lille, Lille, France, and* [5]*Lipid Metabolism DPU, GlaxoSmithKline R&D, Les Ulis, France*

Correspondence
Professor B Staels, Inserm U1011, Institut Pasteur de Lille, 1 rue du Prof Calmette, BP 245, 59019 Lille, France. E-mail: bart.staels@pasteur-lille.fr

Keywords
peroxisome proliferator-activated receptor; lipid metabolism; gene regulation; humanized mouse

Received
24 September 2010
Revised
25 January 2011
Accepted
28 February 2011

BACKGROUND AND PURPOSE

Humanized mice for the nuclear receptor peroxisome proliferator-activated receptor δ (PPARδ), termed PPARδ knock-in (PPARδ KI) mice, were generated for the investigation of functional differences between mouse and human PPARδ and as tools for early drug efficacy assessment.

EXPERIMENTAL APPROACH

Human PPARδ function in lipid metabolism was assessed at baseline, after fasting or when challenged with the GW0742 compound in mice fed a chow diet or high-fat diet (HFD).

KEY RESULTS

Analysis of PPARδ mRNA levels revealed a hypomorph expression of human PPARδ in liver, macrophages, small intestine and heart, but not in soleus and quadriceps muscles, white adipose tissue and skin. PPARδ KI mice displayed a small decrease of high-density lipoprotein-cholesterol whereas other lipid parameters were unaltered. Plasma metabolic parameters were similar in wild-type and PPARδ KI mice when fed chow or HFD, and following physiological (fasting) and pharmacological (GW0742 compound) activation of PPARδ. Gene expression profiling in liver, soleus muscle and macrophages showed similar gene patterns regulated by mouse and human PPARδ. The anti-inflammatory potential of human PPARδ was also similar to mouse PPARδ in liver and isolated macrophages.

CONCLUSIONS AND IMPLICATIONS

These data indicate that human PPARδ can compensate for mouse PPARδ in the regulation of lipid metabolism and inflammation. Overall, this novel PPARδ KI mouse model shows full responsiveness to pharmacological challenge and represents a useful tool for the preclinical assessment of PPARδ activators with species-specific activity.

Abbreviations

ABCA1, ATP-binding cassette type A1; ES, embryonic stem; GW0742, [4-[[[2-[3-fluoro-4-(trifluoromethyl)phenyl]-4-methyl-5-thiazolyl]methyl]thio]-2-methylphenoxy]acetic acid; HDL-C, high-density lipoprotein-cholesterol; KI, knock-in; LDL-C, low-density lipoprotein-cholesterol; PPAR, peroxisome proliferator-activated receptor; TG, triglyceride; WAT, white adipose tissue

Introduction

Peroxisome proliferator-activated receptors (PPARs) are ligand-activated transcription factors belonging to the nuclear receptor superfamily. Three different PPAR genes (α, δ or β and γ) have been identified, each displaying distinct patterns of tissue distribution and natural and pharmacological ligands, attesting the fact that they perform different functions in different cell types (Gross and Staels, 2007). Of the three isotypes, PPARδ (also called PPARβ or PPARβ/δ) is the

most widely distributed. High expression levels were reported in tissues such as adipose tissue, small intestine, liver, skeletal muscle, heart and macrophages (Escher *et al.*, 2001; Higashiyama *et al.*, 2007; Girroir *et al.*, 2008). In contrast to the PPARα and γ isotypes, an understanding of the physiological role of the PPARδ subtype in humans is lagging behind due to the absence of clinically available PPARδ-selective ligands. The recent identification of PPARδ-selective ligands, concomitant with the development of genetically modified mouse models, has revealed roles for PPARδ in lipid and glucose metabolism, energy expenditure and inflammation (Gross *et al.*, 2005; Barish *et al.*, 2006). As a consequence, PPARδ–selective ligands may be useful for the treatment of dyslipidaemia, obesity and insulin resistance. In humans, the benefit of PPARδ activation on lipid metabolism, via the up-regulation of fatty acid oxydation, was confirmed in early clinical trials (phases I and II) with the GW501516 compound (Sprecher *et al.*, 2007; Risérus *et al.*, 2008), a potent activator of PPARδ (Sznaidman *et al.*, 2003).

The mouse is the most widely used model for physiological and preclinical pharmacological studies. However, some pathways are regulated in a species-specific manner. Species-specific differences in xenobiotic response, for instance, are due to intrinsic differences between the human and mouse constitutive androstane receptor (CAR) (Huang *et al.*, 2004) and pregnane X receptor (Xie *et al.*, 2000). Species differences between human and rodent PPARα activity are also well documented (Gonzalez and Shah, 2008). Sequence differences between the two species are often minor, but sufficient to allow ligand selectivity (Keller *et al.*, 1997) and modulation of gene regulation specificity. Indeed in rodent liver, activation of PPARα induces peroxisome proliferation, hepatomegaly and hepatocarcinogenesis, effects which are not observed in human liver (Lefebvre *et al.*, 2006). A study examining the molecular mechanism of these species differences using a humanized mouse model showed that structural differences between human and mouse PPARα are responsible for the differential susceptibility to the development of hepatocarcinomas (Morimura *et al.*, 2006).

Human and mouse PPARδ proteins share 92% homology in their amino acid sequence, with a few non-conservative modifications in the N-terminal region and the ligand-binding domain (LBD). The pharmacological relevance of these changes has not yet been established. However, differences in the EC_{50} between the two species have been reported for some PPARδ ligands such as for bezafibrate and L-165041 (Ram, 2003). Differences located in the N-terminal region could also account for species variations in gene regulation, as recent studies have indicated that gene specificity is in part driven by the N-terminal region of PPARγ and PPARδ (Hummasti and Tontonoz, 2006; Bugge *et al.*, 2009).

Physiological differences upon PPARδ activation have been reported between species, and notably in the regulation of lipid metabolism. PPARδ ligands increase, up to 50%, high-density lipoprotein-cholesterol (HDL-C) levels in obese and non-obese mice (Leibowitz *et al.*, 2000; van der Veen *et al.*, 2005; Briand *et al.*, 2009). In insulin-resistant obese rhesus monkeys, a more relevant model for the study of human pathologies, PPARδ activation not only increased HDL-C levels, but also decreased low-density lipoprotein-cholesterol (LDL-C) and triglyceride (TG) levels and normalized insulin concentrations (Oliver *et al.*, 2001). Such effects on LDL-C and TG levels were not observed in agonist-treated mice (Leibowitz *et al.*, 2000; van der Veen *et al.*, 2005; Briand *et al.*, 2009). The mechanism by which PPARδ activation raises HDL-C levels is still unclear, but is believed to occur via induction of ApoA1-dependent cholesterol efflux following activation of the cholesterol transporter ATP-binding cassette type A1 (ABCA1) in peripheral tissues and human macrophages (Oliver *et al.*, 2001). However, whether this pathway is also induced by PPARδ ligands in mouse macrophages remains controversial (Lee *et al.*, 2003; Li *et al.*, 2004; van der Veen *et al.*, 2005), suggesting the existence of species differences between human and mouse PPARδ.

The development of humanized mouse models has provided useful tools to explore the functional and regulatory differences between human and mouse orthologous genes. Moreover, humanized mouse models are also valuable tools for preclinical pharmacological evaluation of ligands. In this study, we report the development of a new mouse model humanized for PPARδ, named the PPARδ knock-in (PPARδ KI) mouse. Moreover, we have characterized this model and the role of human PPARδ in lipid metabolism *in vivo* using these mice.

Methods

PPARδ gene targeting

Genomic clones encompassing the 5′ region to exon 3 and 3′ region to exon 8 of the mouse PPARδ gene were obtained by screening a Sv/129 genomic mouse library, generated and kindly provided by A. Bègue (Institut de Biology de Lille, France). The targeting vector was constructed using PCR amplification introducing new cloning sites in the human cDNA. A *Nco*I site was generated upstream of the start codon by modifying one base before the ATG. The human PPARδ cDNA was inserted between the newly generated *Nco*I site and the *Bgl*II site located a few base pairs upstream of the stop codon at the end of the exon 8. This results in the replacement of the coding region only. A neomycin cassette flanked by two loxP sites was introduced into the intron sequence upstream of the human cDNA. The targeting vector contained 1.7 kb of homologous sequence 5′ of the neomycin cassette and 6.3 kb of homologous sequence 3′ of the human PPARδ cDNA (Figure 1A). A herpes simplex virus thymidine kinase gene was inserted at the 3′ end of the construct for negative selection against random insertion of the targeting vector.

Targeting of the constructs to obtain heterozygous embryonic stem (ES) cells was performed using standard procedures (Lee *et al.*, 1995). After positive and negative selection, homologous recombination of the ES clones was verified by Southern blot analysis using 5′ and 3′ probes (Figure 1B). One of the three positive ES clones microinjected into C57BL/6J blastocysts generated chimeric mice with ~60% agouti coat colour.

Chimeric mice with germ line transmission were obtained by breeding with C57BL/6J mice. The transmission of the modified allele was monitored by Southern blot analysis with the 5′ probe and *BamH*I digestion in the first generation of the progenies. Genotypes of subsequent generations were

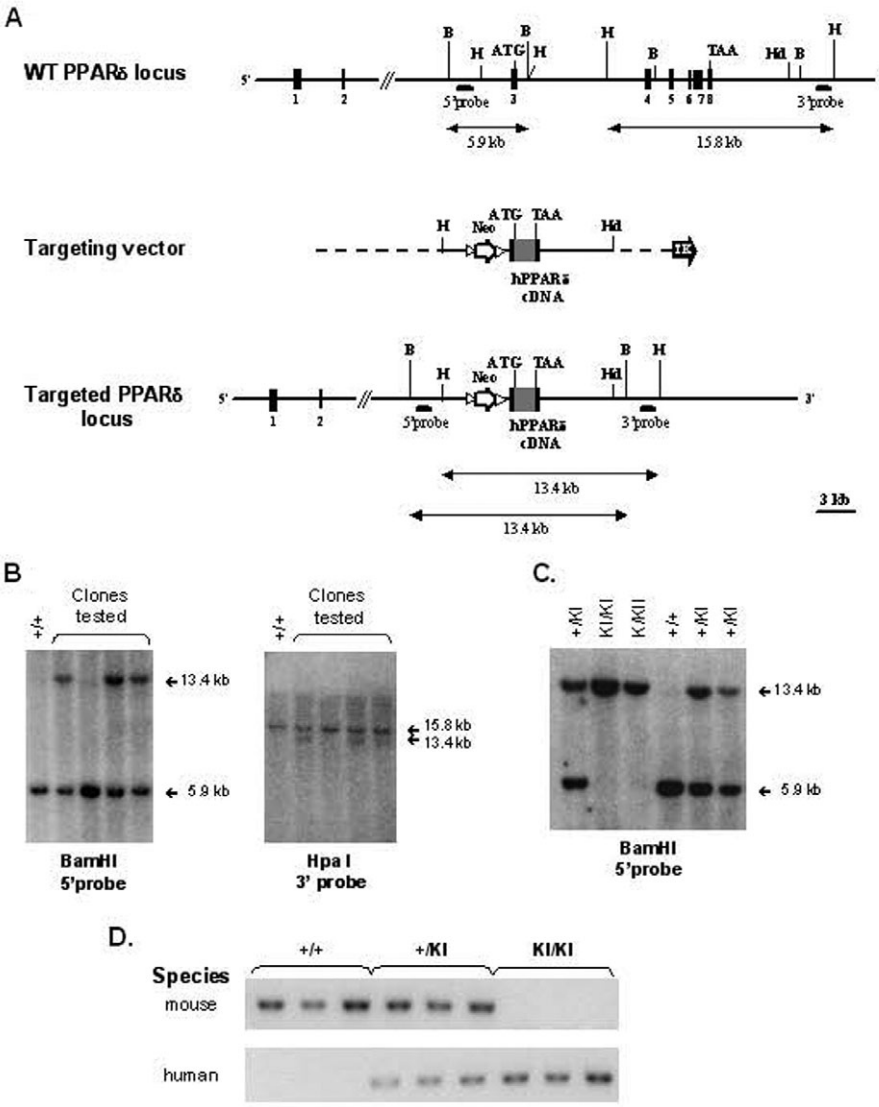

Figure 1

Targeted replacement of the mouse PPARδ gene by the human orthologous cDNA. (A) Strategy for the development of the PPARδ KI mouse model. From top to bottom: wild-type locus of the mouse PPARδ gene with the coding sequence initiating in exon 3 and ending in exon 8, the targeting vector and the targeted locus. Expected DNA restriction fragments and their size are represented by double-headed arrows under the respective genomic structures. Restriction sites are: B, *BamH*I; H, *Hpa*I; Hd, *Hind*III. Black boxes indicate exons, grey boxes the cDNA, arrow heads loxP sites, black arrow the thymidine kinase (TK) expression cassette, open arrow the neomycin (Neo) expression cassette. (B) Genomic Southern blot analysis of four targeted embryonic stem cell clones (recombinant ES clones) as opposed to wild-type cells (+/+). Southern blots show integration of the targeting vector with appropriate genomic alterations at 5′ and 3′ termini to the homologous recombination sites. When one allele of the mouse PPARδ gene is replaced by homologous recombination, *BamH*I and *Hpa*I restriction fragments of 13.4 kb appeared when the gene was analysed with the 5′ probe and 3′ probe respectively. (C) Southern blot analysis of tail DNA from wild-type (+/+), heterozygous (+/KI) and homozygous (KI/KI) mutant mice carrying either the wild-type, one or both targeted alleles. Deduced genotypes are indicated on top. (D) RT-PCR with species-specific primers performed on liver samples from wild-type (+/+), heterozygous (+/KI) and homozygous (KI/KI) PPARδ KI mice. ES, embryonic stem; KI, knock-in.

determined by PCR. Mice were backcrossed 10 generations in order to obtain a C57BL/6J-stabilized genetic background.

RNA extraction and quantitative PCR analysis

Tissue RNA isolation and quantitative PCR analysis were performed as previously described (Lalloyer *et al.*, 2009). Results are expressed normalized to 36B4 or cyclophilin.

Analysis of human and mouse PPARδ transcripts

In order to verify the replacement of mouse PPARδ coding sequence by the human orthologous cDNA, a RT-PCR analysis was performed with a set of primers with the forward primer specific to each species (human forward: 5′AGAAAG AGGAAGTGGCAGA3′, mouse forward: 5′AGAAAGAGGAA

GTGGCCAT3′) and the reverse primer located in a region homologous between the two species (common reverse: 5′GAGAAGGCCTTCAGGTCG3′). The species-specific forward primers displayed mismatches in their 3′ region. In order to reduce cross-reaction of the species-specific primers, the annealing temperature was set at 66°C. PCR amplification products were separated on an agarose gel stained with ethidium bromide and visualized under UV light.

Animal experiments

All animal care and experimental procedures complied with the European Community specifications (Council Directives 86/609/EEC) regarding the use of laboratory animals and were approved by the Pasteur Institute of Lille Animal facilities (licence number B59-35009) and The Nord-Pas de Calais Ethical Committee for animal use. Homozygous PPARδ KI and wild-type (WT) littermates used for fasting and high-fat diet (HFD) studies were of mixed background Sv129/C57BL/6J. Studies with chow diet were performed using 10 generation back-crossed homozygous PPARδ KI C57BL/6J mice. C57BL/6J mice used for backcrossing and as controls for GW0742 treatment were from a commercial source (Iffa Credo, France). Mice were group housed and given access to chow diet and water *ad libitum*.

Wild-type control and PPARδ KI mice (7–15 weeks of age) were matched according to weight, glycaemia and cholesterol levels. Mice were fed either a standard chow diet or an HFD containing 35.5% (w/w) fat manufactured by Safe (Augy, France) as described by Luo *et al*. (1998). Mice were treated with the GW0742 compound (Sznaidman *et al*., 2003) (in 0.5% hydroxypropyl methyl cellulose, 1% Tween 80, pH 3.2) at the dose of 10 $mg \cdot kg^{-1}$ or vehicle by oral gavage twice a day for 14 days. On the day they were killed, mice were deprived of food for 6 h. For the fasting experiment, food was withdrawn for 24 h. Blood was collected by retro-orbital venipuncture under isoflurane anaesthesia. Mice were killed by cervical dislocation and tissues were harvested, flash frozen and stored at –80°C until required.

Plasma metabolite analysis

Plasma lipid concentrations were determined in mice deprived of food for 6 or 24 h. Glycaemia was determined using Glucotrend (Roche). Retro-orbital blood samples were drawn in EDTA-coated tubes at death. Plasma was separated by low-speed centrifugation and kept at 4°C or frozen. Plasma free fatty acids (FFAs), β-hydroxybutyrate, lactate were determined using kits from Wako, Randox Laboratories and Trinity Biotech, respectively.

Cholesterol and TG concentrations were determined by enzymatic assays using commercially available reagents (Biomerieux, France). Lipids of individual plasma samples were separated by fast protein liquid chromatography (FPLC) by gel filtration onto a Sepharose 6 10/300 GL column (GE Healthcare) with online cholesterol and TG determination. This system allows separation of the three major lipoprotein classes – VLDL, LDL and HDL.

Macrophage isolation

Peritoneal macrophages were isolated from WT and PPARδ KI mice 3 days after a thioglycolate challenge. Macrophages were cultured in RPMI 1640 medium and 10% FBS for 24 h followed by a 12 h starvation period in medium with 0.2% FBS prior to treatment. Macrophages were treated during 24 h with vehicle or GW0742 at 100 nM. The inflammatory response was studied in macrophages treated with LPS (Sigma) at 100 $ng \cdot mL^{-1}$ for 24 h in the presence of vehicle or GW0742 at 100 nM.

Statistical analysis

Differences between two groups were compared with Student's unpaired two-tailed *t*-test. Multiple comparison was performed with one-way ANOVA. Significant differences were subjected to *post hoc* analysis using the Tukey's test. A *P*-value of 0.05 or less was considered statistically significant. Calculations were performed using Graphpad Prism software.

Results

Gene replacement of the mouse PPARδ gene with the human PPARδ cDNA

The targeting strategy used for the development of the humanized PPARδ mouse is illustrated in Figure 1A. In brief, the mouse PPARδ coding region, spanning from the start codon in exon 3 to the stop codon in exon 8, was replaced with the cDNA of the human orthologous gene through homologous recombination in ES cells. Homologous recombination between the endogenous mouse PPARδ locus and the targeting construct results in a chimeric gene in which all the mouse protein coding sequences have been replaced with sequences coding for human PPARδ. This chimeric gene, called targeted locus, retains all the mouse regulatory elements of the promoter region as well as the 5′ and 3′UTR.

Recombinant ES clones were positively and negatively selected against neomycin and thymidine kinase activity, respectively. Successful integration and replacement with the human PPARδ cDNA was confirmed by Southern blot analysis with 5′ and 3′ probes (Figure 1B). The targeted locus was transmitted to the F1 generation from chimera mice that were obtained from one of the targeted cell lines (Figure 1C). Humanized homozygote mice (PPARδ KI) were born at predicted Mendelian frequencies, appeared grossly normal and produced normal progeny. No weight and size differences were observed during the lifespan of the PPARδ KI mice.

Analysis of human PPARδ expression level

Successful replacement and expression of human PPARδ was monitored in liver by RT-PCR using species-selective primers (Figure 1D). Human PPARδ mRNAs were detected in heterozygous and homozygous PPARδ KI mice, whereas mouse PPARδ mRNA was absent in homozygous PPARδ KI mice. Northern blot analysis, using a common probe located downstream of the stop codon in the 3′UTR, indicated that a full length mRNA was processed from the chimeric human PPARδ gene (Figure S1). mRNA expression levels of human PPARδ were determined by quantitative PCR in several tissues in which PPARδ is metabolically active. Using primers located in the common 5′UTR, and when compared with mouse PPARδ mRNA levels, human PPARδ transcript levels were found to be lower in a number of tissues such as liver, macrophages, small intestine

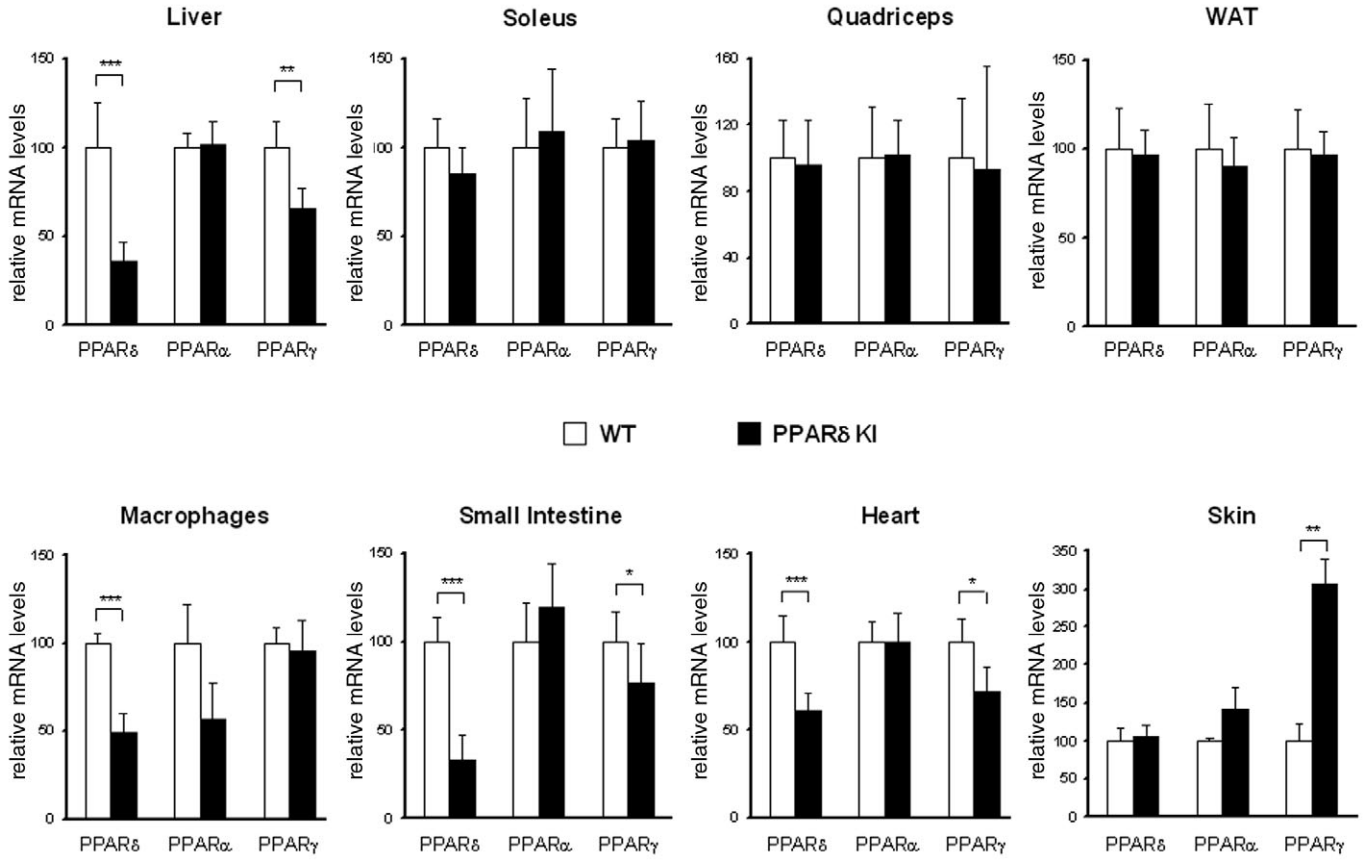

Figure 2

Comparative expression analysis of the different PPAR isotypes in PPARδ KI and wild-type (WT) mouse tissues. Transcript levels of PPARδ, PPARα and PPARγ were measured in liver, skeletal muscle (soleus and quadriceps), white adipose tissue (WAT), peritoneal macrophages, small intestine, heart and skin. Relative expression of PPAR transcripts in WT and PPARδ KI mice was measured by quantitative PCR. Expression values are normalized to 36B4 and expression of PPARδ, PPARα and PPARγ in WT mice was set at 100 for each tissue. Values represent means ± SD. Significant differences by Student's *t*-test. **P* < 0.05; ***P* < 0.005; ****P* < 0.001 WT versus PPARδ KI. KI, knock-in.

and heart (Figure 2). In contrast, hPPARδ expression was similar in white adipose tissue (WAT), skin and soleus (rich in oxidative fibre types and expressing high levels of PPARδ) and quadriceps (composed of mixed oxidative and glycolytic fibre types and expressing lower PPARδ levels) muscles. Levels of PPARα and PPARγ transcripts were also analysed in order to detect compensatory mechanisms triggered by the replacement of mouse PPARδ and down-regulation of hPPARδ expression, as previously shown in PPARα null mice (Muoio *et al.*, 2002). PPARα mRNA levels were similar between WT and PPARδ KI mice, except for a statistically non-significant decrease in macrophages (Figure 2). PPARγ mRNA levels in PPARδ KI mice were similar in skeletal muscles, WAT and macrophages but were lower in liver, small intestine and heart and strongly elevated in skin (Figure 2).

Analysis of plasma lipids in chow fed mice

Serum lipid concentrations and distributions were analysed in adult, female and male, mice at the age of 10 weeks. In males, serum cholesterol levels were significantly lower (13%) in PPARδ KI mice compared with WT controls (Table 1 and Figure S2A). Analysis of the lipid distribution profiles indicated that the reduction of cholesterol occurred in the HDL fraction. Similarly, in females, total cholesterol and HDL-C were 18% lower in PPARδ KI mice when compared with WT mice (Table 1), although this did not reach statistical significance. Analysis of TG levels did not show significant differences between WT and PPARδ KI mice in both female and male mice (Table 1 and Figure S2B). Glycaemia in mice was similar between male WT and PPARδ KI mice (2.03 ± 0.35 g·L^{-1} vs 2.12 ± 0.26 g·L^{-1}, respectively), whereas in female mice glycaemia was significantly lower (17%) in PPARδ KI versus WT mice (1.78 ± 0.37 g·L^{-1} vs. 2.15 ± 0.32 g·L^{-1}, respectively, $P = 0.007$).

hPPARδ did not alter metabolic parameters during fasting

As PPARδ acts as a fatty acid sensor and is activated during adaptive responses to fasting or exercise (Sanderson *et al.*, 2009), the response of PPARδ KI mice to 24 h fasting was tested next.

As expected, an increase of FFAs and β-hydroxybutyrate and a decrease of lactate, TG and blood glucose was observed in WT mice after a 24 h fasting period (Figure 3A).

Table 1

Lipid profiles of WT and PPARδ KI mice on chow diet

Genotype		Male WT (n = 22)	PPARδ KI (n = 28)	Female WT (n = 10)	PPARδ KI (n = 16)
Cholesterol (g L^{-1})	Total	1.09 ± 0.25	0.94 ± 0.20**	0.91 ± 0.15	0.75 ± 0.29
	VLDL	0.04 ± 0.02	0.04 ± 0.02	0.02 ± 0.02	0.01 ± 0.02
	LDL	0.15 ± 0.05	0.14 ± 0.04	0.10 ± 0.05	0.09 ± 0.05
	HDL	0.90 ± 0.20	0.76 ± 0.18**	0.80 ± 0.12	0.65 ± 0.25
Triglycerides (g L^{-1})	Total	1.20 ± 0.38	1.29 ± 0.33	1.04 ± 0.49	0.95 ± 0.37
	VLDL	0.47 ± 0.20	0.44 ± 0.22	0.35 ± 0.14	0.28 ± 0.18
	LDL	0.21 ± 0.07	0.18 ± 0.07	0.11 ± 0.03	0.10 ± 0.04
	HDL	0.09 ± 0.04	0.07 ± 0.08	0.14 ± 0.11	0.12 ± 0.06

Plasma lipoproteins of 10 week-old male and female WT and PPARδ KI mice fed a chow diet were individually separated according to their size by FPLC. Values represent means ± SD. Significant differences by Student's t-test *P < 0.05; **P < 0.005***P < 0.001 WT vs PPARδ KI. FPLC, fast protein liquid chromatography; HDL, high-density lipoprotein; LDL, low-density lipoprotein; VLDL, very low-density lipoprotein.

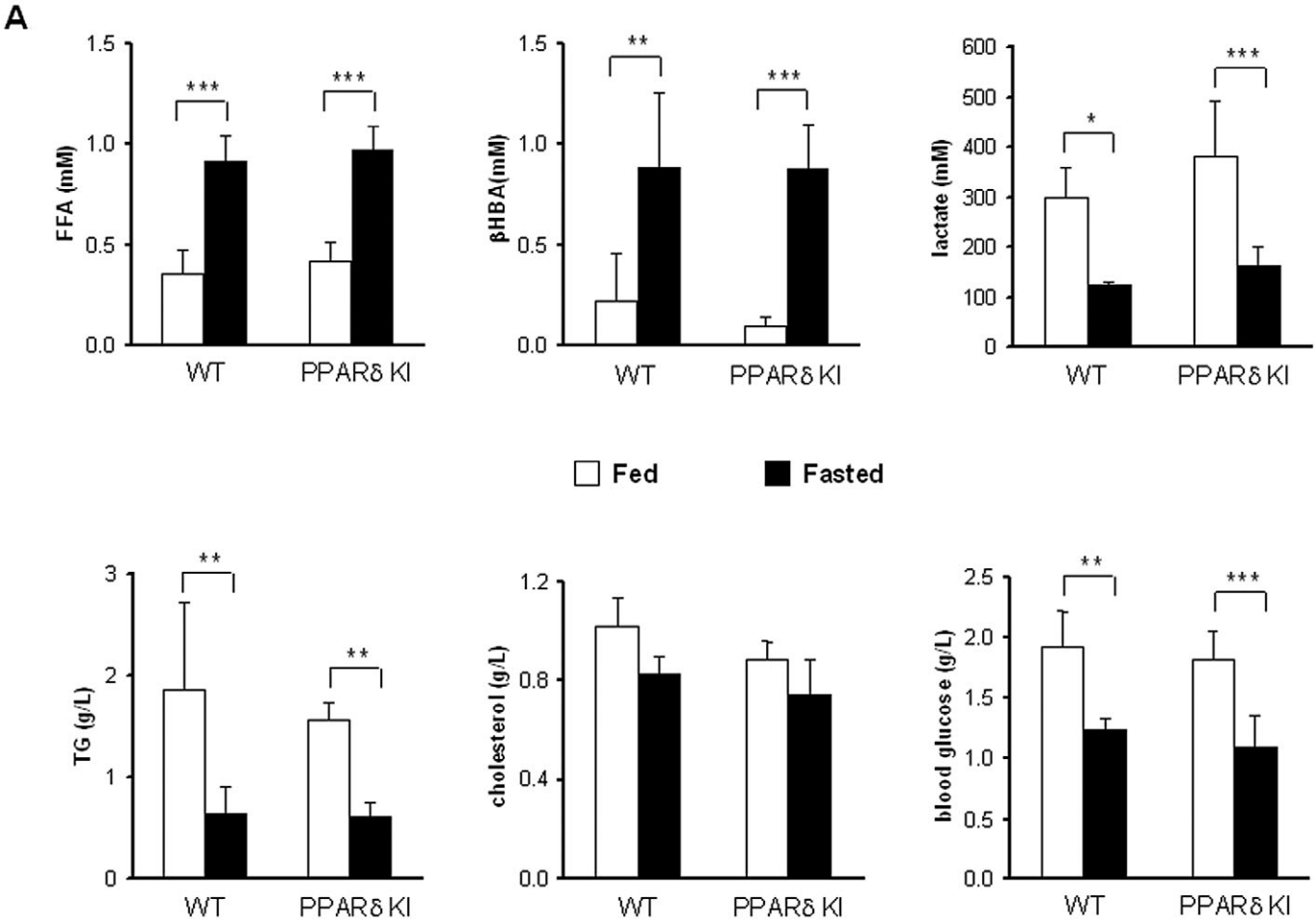

Figure 3

Expression of hPPARδ did not alter the metabolic response to fasting. (A) Plasma metabolites were analysed in fed, 24 h fasted wild-type and PPARδ KI mice. (B) Expression of genes involved in carbohydrate, lipid and lipoprotein metabolism were measured by quantitative PCR in livers from fed and fasted wild-type and PPARδ KI mice. Expression values are normalized to cyclophilin and expression of fed wild-type mice was set at 100. Values represent means ± SD. Significant differences by one-way ANOVA analysis. *P < 0.05; **P < 0.005; ***P < 0.001 fed versus fasted. KI, knock-in.

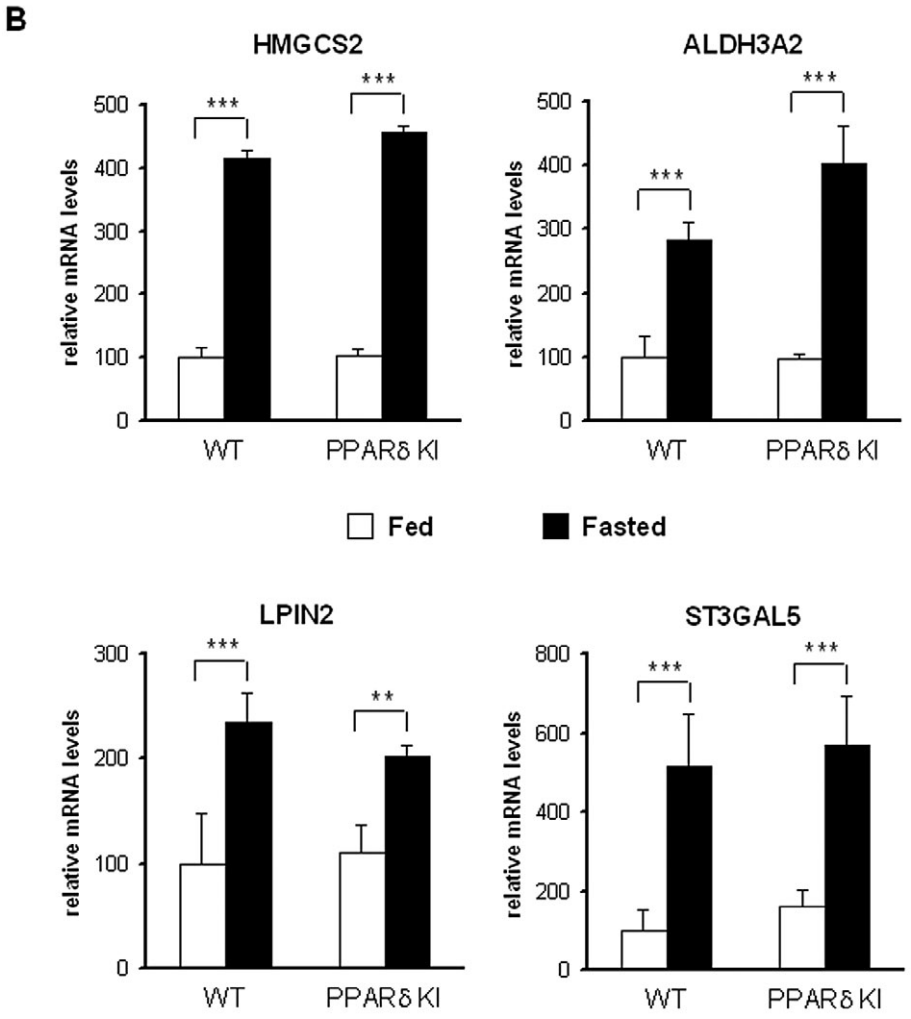

Figure 3
Continued.

Cholesterol levels did not change upon fasting in WT mice. PPARδ KI mice displayed a similar response to WT mice. Similarly, at the transcriptional level, mRNA levels the ketogenic enzyme, 3-hydroxy-3-methylglutaryl-CoA synthase 2 (HMGCS 2), a PPAR target gene, and aldehyde dehydrogenase 3 family, member A2 (ALDH3 A2), a specific PPARα target gene thus reflecting PPARα activity (Sanderson *et al.*, 2009), were induced by fasting in both WT and PPARδ KI mice (Figure 3B). Hepatic mRNA levels of fasting-regulated PPARδ target genes such as lipin 2 (LPIN2) and ST3 β-galactoside α-2,3-sialyltransferase 5 (ST3GAL5) (Sanderson *et al.*, 2009) were regulated in a similar manner in WT and PPARδ KI mice during fasting (Figure 3B). These results indicate that the response of PPARδ-selective genes, as well as PPARα-selective genes, is similar between PPARδ KI and WT mice upon fasting.

Effect of GW0742 treatment on plasma lipids and lipid gene regulation

The effect of hPPARδ activation on lipid and glucose metabolism was assessed in male WT and PPARδ KI mice fed a standard chow diet and treated with the PPARδ-selective activator GW0742 (Sznaidman *et al.*, 2003) for 14 days at a dose of 20 $mg \cdot kg^{-1} \cdot day^{-1}$. Treatment with GW0742 did not alter body weight of either WT and PPARδ KI mice but increased liver weight by 26% and 40% in WT and PPARδ KI mice, respectively (Table 2), probably due to the induction of peroxisome proliferation (van der Veen *et al.*, 2005). GW0742 treatment did not alter blood glucose concentration in either genotype (Table 2).

GW0742 treatment significantly increased total cholesterol in WT (24%) and PPARδ KI mice (33 %) (Table 3). FPLC profile analysis of plasma lipids indicated that this rise was essentially caused by an increased cholesterol content in HDL and LDL particles (Table 3 and Figure S3A). In WT mice the HDL-C and LDL-C increase was 19% and 64%, whereas in PPARδ KI mice the increase was 31% and 40%, respectively. The variations in response between WT and PPARδ KI mice were not statistically, significantly different.

Gene expression levels of genes involved in HDL metabolism were assessed in liver, a major tissue involved in lipid

Table 2

Effect of GW0742 treatment on liver weight and blood glucose of WT and PPARδ KI male mice

Genotype	WT Vehicle	WT GW0742	PPARδ KI Vehicle	PPARδ KI GW0742
Liver weight (% of body weight)	4.62 ± 0.30	5.85 ± 0.34***	4.13 ± 0.28	5.76 ± 0.61***
Blood glucose (g L^{-1})	2.01 ± 0.22	1.97 ± 0.20	2.04 ± 0.42	2.04 ± 0.25

Mice were treated by oral gavage with GW0742 (20 mg·kg^{-1}·day^{-1}) or vehicle alone for 14 days (n = 8 per group). Values represent means ± SD. Significant differences by one-way ANOVA analysis, *P < 0.05; **P < 0.005; ***P < 0.001 vehicle versus GW0742.

Table 3

Influence of GW0742 treatment on lipid profiles of WT and PPARδ KI male mice

Genotype		WT Vehicle	WT GW0742	PPARδ KI Vehicle	PPARδ KI GW0742
Cholesterol (g L^{-1})	Total	1.10 ± 0.11	1.37 ± 0.08***	1.03 ± 0.07	1.37 ± 0.10***
	VLDL	0.05 ± 0.03	0.05 ± 0.02	0.04 ± 0.02	0.05 ± 0.01
	LDL	0.14 ± 0.03	0.23 ± 0.06***	0.15 ± 0.02	0.21 ± 0.04*
	HDL	0.89 ± 0.09	1.06 ± 0.04***	0.82 ± 0.05	1.08 ± 0.10***
Triglycerides (g L^{-1})	Total	1.00 ± 0.39	0.94 ± 0.23	0.94 ± 0.20	0.89 ± 0.17
	VLDL	0.39 ± 0.25	0.41 ± 0.16	0.38 ± 0.18	0.34 ± 0.15
	LDL	0.14 ± 0.04	0.07 ± 0.01**	0.11 ± 0.05	0.07 ± 0.02*
	HDL	0.08 ± 0.05	0.08 ± 0.04	0.07 ± 0.03	0.09 ± 0.06

Mice were treated by oral gavage with GW0742 (20 mg·kg^{-1}·day^{-1}) or vehicle alone for 14 days (n = 8 per group). Plasma lipoproteins were individually separated according to their size by FPLC. Values represent means ± SD. Significant differences by one-way ANOVA analysis, *P < 0.05; **P < 0.005; ***P < 0.001 vehicle versus GW0742. FPLC, fast protein liquid chromatography; HDL, high-density lipoprotein; VLDL, very low-density lipoprotein.

and lipoprotein metabolism. mRNA expression levels of the scavenger receptor B1, an HDL receptor, and the ABCA1 transporter protein, which regulates ApoA1-dependent cholesterol efflux and HDL formation, were not modified in treated mice from either genotype (Figure 4A and data not shown). The genes of the two major HDL apolipoproteins, APOA1 and APOA2, were not regulated either (data not shown). Among the genes involved in HDL remodelling, PLTP, which catalyses the transfer of phospholipids from VLDL to HDL and between HDL particles, was up-regulated upon GW0742 treatment in both WT and PPARδ KI mice (Figure 4A).

Analysis of genes involved in LDL metabolism such as the LDL-receptor, LDL-R, did not reveal an effect of GW0742 in WT and PPARδ KI mice (data not shown). By contrast, mRNA of APOB, the major apolipoprotein of LDL, was slightly down-regulated in PPARδ KI-treated mice only (Figure 4A). The physiological significance of this differential regulation is not known.

GW0742 treatment did not alter total TG levels in either WT or PPARδ KI mice. Interestingly, FPLC separation of the lipoprotein fractions indicated a decrease of 50% and 36% in TG content of LDL particles in WT- and PPARδ KI-treated mice, respectively. This decrease was not detected in the total pool as the TG content of LDL particles only represents a minor percentage of total TG (Table 3 and Figure S3B). The decreased TG levels in LDL particles upon GW0742 treatment in WT and PPARδ KI mice was associated with a fourfold increase in mRNA levels of lipoprotein lipase (LPL) and a 30% decrease in the LPL inhibitors, apolipoprotein C3 (APOC3) and angiopoietin-like 3 (ANGPTL3) in liver (Figure 4A). In addition, mRNA levels of pyruvate dehydrogenase kinase 4 (PDK4), an inhibitor of the pyruvate dehydrogenase complex, were strongly up-regulated in WT and PPARδ KI mice (Figure 4B). The regulation of these genes was not significantly different between WT and PPARδ KI mice.

In addition, the regulation of genes involved in intrahepatic lipid metabolism including fatty acid β-oxidation, storage and transport, was analysed. GW0742 treatment induced in both genotypes an increase in the mRNA levels of acyl-CoA oxidase (ACO), carnitine palmitoyltransferase 1b (CPT1b), liver-fatty acid binding protein (L-FABP), liver-fatty acid transport protein (L-FATP) and CD36 (Figure 4B). Interestingly, the up-regulation of ACO, L-FATP and CD36, but not CPT1b or L-FABP, was slightly, albeit significantly lower in PPARδ KI-treated versus WT-treated mice.

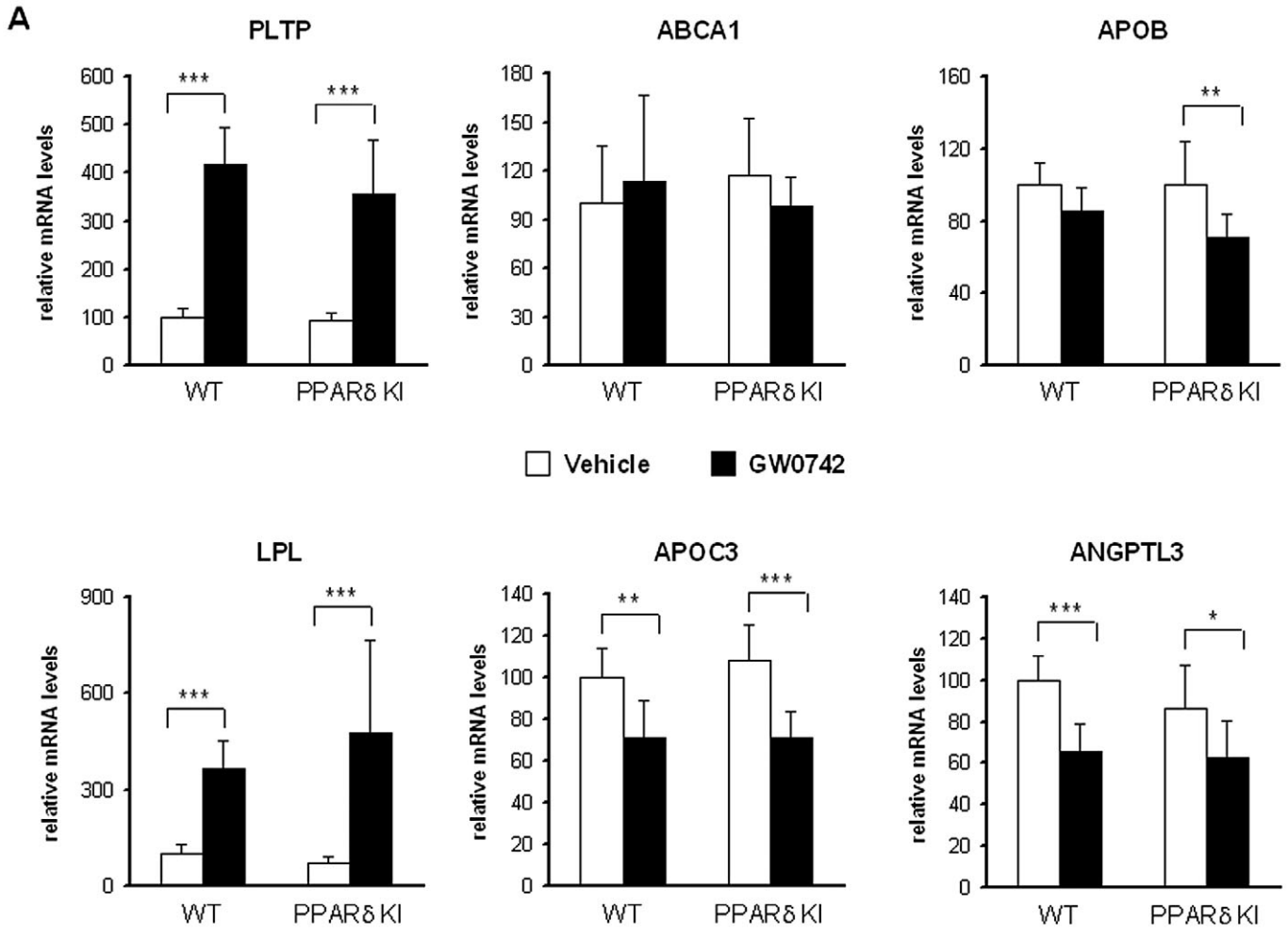

Figure 4

Effect of GW0742 treatment on gene regulation in livers of wild-type (WT) and PPARδ KI mice. Liver mRNA expression levels from vehicle- and GW0742-treated WT and PPARδ KI mice were measured by quantitative PCR. Analysed transcript were classified according to their metabolic function: (A) lipoprotein and TG metabolism (B) fatty acid oxidation and transport. Expression values are normalized to cyclophilin and expression of vehicle-treated WT mice was set at 100. Values represent means ± SD. Significant differences by one-way ANOVA analysis. *$P < 0.05$; **$P < 0.005$; ***$P < 0.001$ vehicle versus GW0742. #$P < 0.05$; ##$P < 0.005$ ###$P < 0.001$ WT versus PPARδ KI. KI, knock-in; TG, triglyceride.

Gene expression of ABCA1, uncoupling protein 2 and angiopoietin-like 4 is up-regulated by mouse and human PPARδ in skeletal muscle

PPARδ is highly expressed in oxidative type I muscle fibres (Muoio *et al.*, 2002; Wang *et al.*, 2004) and plays a predominant role in fatty acid oxidation in skeletal muscle by regulating mitochondrial gene expression of enzymes of fatty acid oxidation (Ehrenborg and Krook, 2009). mRNA levels of fatty acid oxidation and lipid handling genes were thus analysed in the soleus muscle, mainly constituted of oxidative type I muscle fibres (Dressel *et al.*, 2003; Wang *et al.*, 2004). Surprisingly, mRNA levels of CPT1b, CD36, PDK4, uncoupling protein 3 (UCP3), L-FATP, glucose transporter type 4 (GLUT4) and PPARγ coactivator 1α (PGC1α), which have been described previously as PPARδ regulated genes in muscle (Dressel *et al.*, 2003; Tanaka *et al.*, 2003; Sprecher *et al.*, 2007), were not changed upon GW0742 treatment in either WT or PPARδ KI mice (Figure 5), and data not shown. By contrast, the ABCA1, uncoupling protein 2 (UCP2) and angiopoietin-like 4 (ANGPTL4) transcripts were up-regulated to the same extent in WT- and PPARδ KI-treated mice (Figure 5).

Effect of GW0742 on metabolic parameters and inflammation in high-fat diet-fed mice

As PPARδ activation has been shown to prevent diet-induced obesity, the response of PPARδ KI mice to high-fat diet (HFD) feeding was assessed. Mice were fed 7 weeks with a HFD prior to 14 days treatment with the GW0742 compound. During the 7 weeks of HFD feeding, weight gain and plasma metabolic parameters (TG, cholesterol, glucose and insulin) were similar in both genotypes (Figure S4A, and data not shown).

Fourteen-day treatment with GW0742 did not modify weight or blood glucose and plasma insulin levels in both

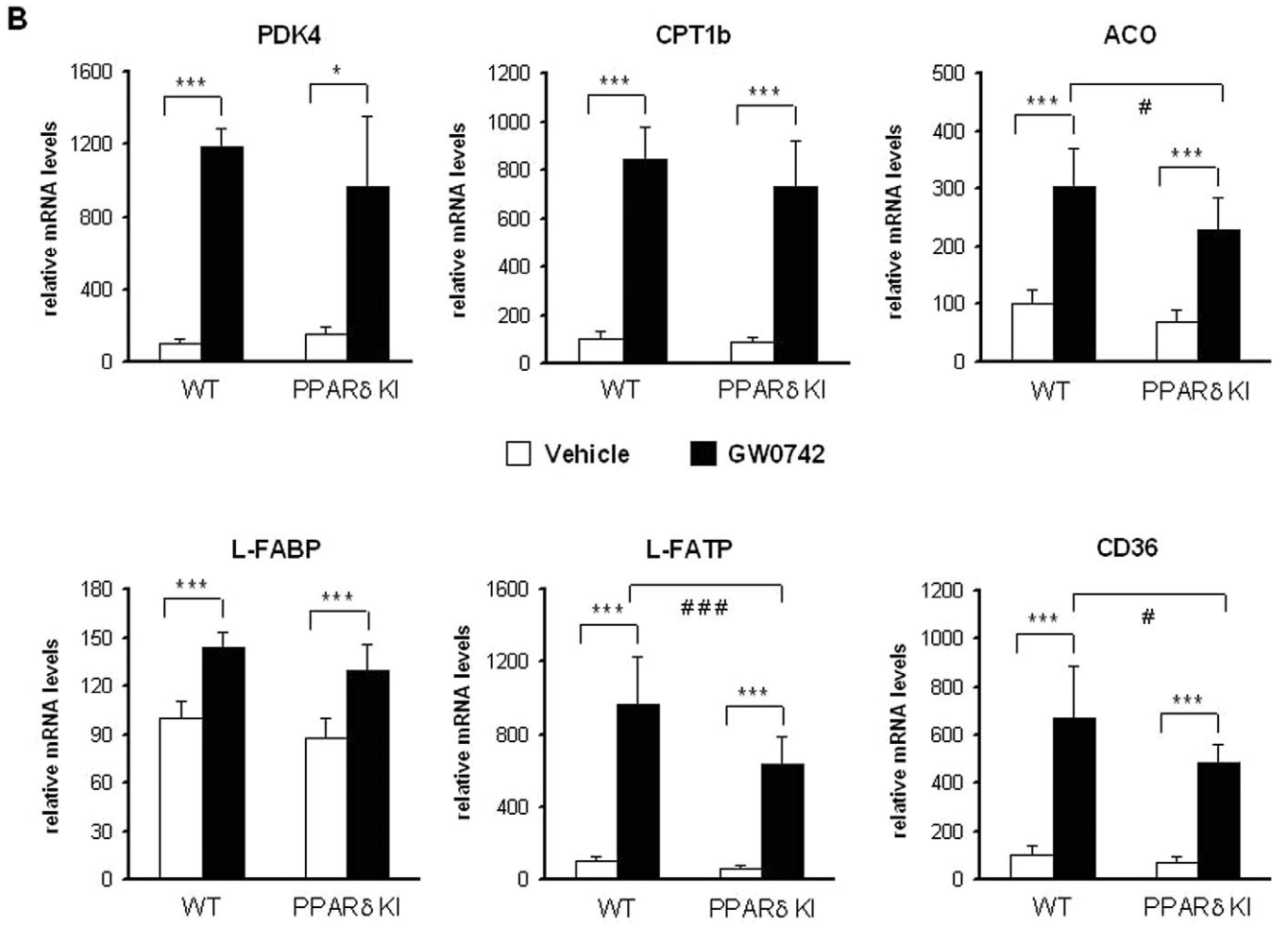

Figure 4

Continued.

WT and PPARδ KI mice (Figure S4B). GW0742 treatment increased liver weight size similarly in WT and PPARδ KI mice (Figure S4B). GW0742 treatment increased total and HDL-cholesterol levels to a similar extent in WT and PPARδ KI mice (Figure 6A). Plasma TG did not change upon GW0742 treatment in both WT and PPARδ KI mice (Figure 6A). mRNA levels of genes involved in lipid and lipoprotein metabolism, including ACO, and CD36 were similarly regulated upon GW0742 treatment in both WT and PPARδ KI mice, whereas mRNA of PLTP up-regulation was slightly weaker in PPARδ KI-treated mice compared with WT-treated mice (Figure 6B).

High-fat diet feeding causes liver steatosis and inflammation. Expression of acute response genes in hepatocytes such as fibrinogen-α and fibrinogen-β was down-regulated in a similar manner in both WT and PPARδ KI mice following GW0742 treatment (Figure 6C). Regulation of the inflammatory response by PPARδ in Kupffer cells, the resident hepatic macrophages, was also investigated. Transcription of cytokines such as TNFα and IL-1 receptor antagonist-a (IL-1Ra) were down-regulated and up-regulated, respectively, upon GW0742 treatment to a similar extent in WT and PPARδ KI mice. mRNA levels of specific markers of alternative macrophage activation, such as dectin-1 (CLEC7A) and arginase 1 (ARG1), were similarly down-regulated by GW0742 in WT and PPARδ KI mice (Figure 6C). These results are in contradiction with those of Odegaard *et al.* showing a strong induction of mRNA levels of CLEC7A and ARG1 by GW0742 (Odegaard *et al.*, 2008) in Sv129/SvJ mice. This discrepancy could be caused by different mouse genetic background used for the studies.

Response of hPPARδ to GW0742 in macrophages

Peroxisome proliferator-activated receptor δ represents the major PPAR isotype in human and mouse macrophages (Vosper *et al.*, 2001; Lee *et al.*, 2003); and acts as a modulator of the inflammatory response (Lee *et al.*, 2003; Welch *et al.*, 2003) and as a VLDL sensor (Chawla *et al.*, 2003; Lee *et al.*, 2006).

At first, regulation of genes involved in the inflammatory response by hPPARδ was assessed in LPS-stimulated peritoneal macrophages treated with GW0742 at 100 nM. LPS stimulation of cells was accompanied by a strong increase in mRNA levels of iNOS and MCP1, although this increase was weaker and stronger, respectively, in macrophages of PPARδ KI when compared with WT macrophages (Figure 7A), probably as a

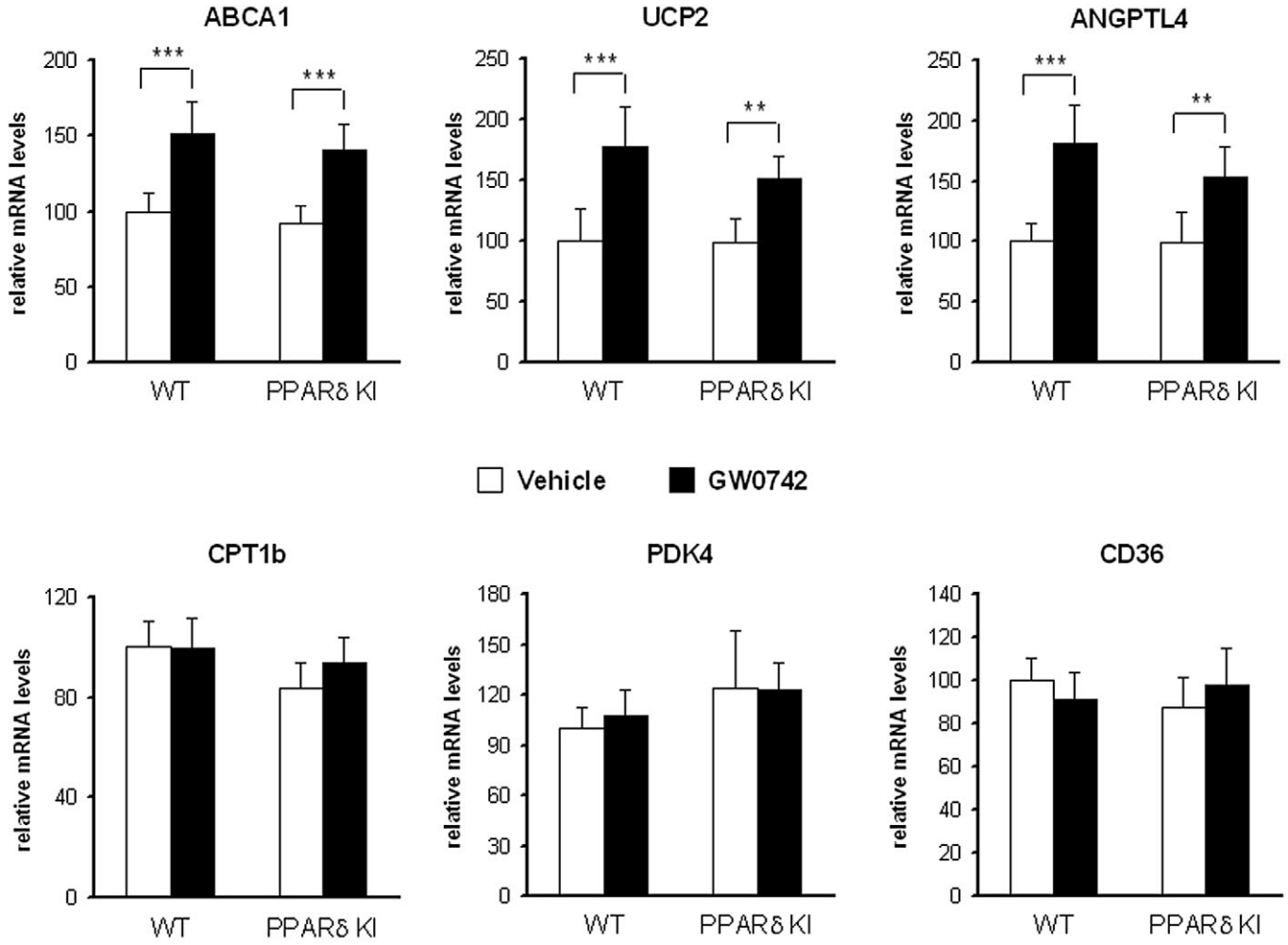

Figure 5

Effect of GW0742 treatment on gene regulation in soleus muscle of wild-type and PPARδ KI mice. mRNA expression levels of vehicle- and GW0742-treated wild-type and PPARδ KI mice were measured by quantitative PCR. Expression values are normalized to 36B4 and expression of vehicle-treated wild-type mice was set at 100. Values represent means ± SD. Significant differences by one-way ANOVA analysis. *$P < 0.05$; **$P < 0.005$; ***$P < 0.001$ vehicle versus GW0742. KI, knock-in.

consequence of reduced hPPARδ mRNA levels (Figure 2). However, GW0742 stimulation resulted in a similar decrease in LPS-induced mRNA levels of iNOS and MCP1 between macrophages of WT and PPARδ KI mice (Figure 7A).

Human–mouse dissimilarities have been observed in the regulation of the transcription of some genes involved in lipid homeostasis in macrophages in response to PPARδ ligands, such as ABCA1, liver X receptor α (LXRα) and the lipid transporter A-FABP (Oliver *et al.*, 2001; Vosper *et al.*, 2001; Lee *et al.*, 2003; Li *et al.*, 2004). To determine whether the PPARδ protein sequence is involved in these species-specific regulations, mRNA levels of these genes were analysed in peritoneal macrophages treated with GW0742 (100 nM). No significant regulation of mRNA levels was detected for ABCA1, LXRα and A-FABP upon GW0742-treatment in macrophages of WT- and PPARδ KI-treated mice (Figure 7B). By contrast, mRNA levels of CPT1a, CD36 and adipophilin (ADRP), were up-regulated to a similar extent in WT- and PPARδ KI-treated mice (Figure 7B), demonstrating the efficacy of the GW0742 treatment. Interestingly, the expression level of CPT1a was significantly lower in untreated macrophages of PPARδ KI compared with WT mice. Furthermore, the increase in CPT1a and ADRP mRNA induced was significantly lower in PPARδ KI- versus WT-treated mice, this might be due to the lower expression level of hPPARδ in macrophages (Figure 2).

Discussion

Species differences in the response to PPARδ activation between mouse and humans can be attributed to factors such as differences in protein sequence between the species, different expression levels of PPARδ in the tissues, relative binding affinities for the heterodimerization partner RXR, differences in the PPREs in the promoters of its target genes,

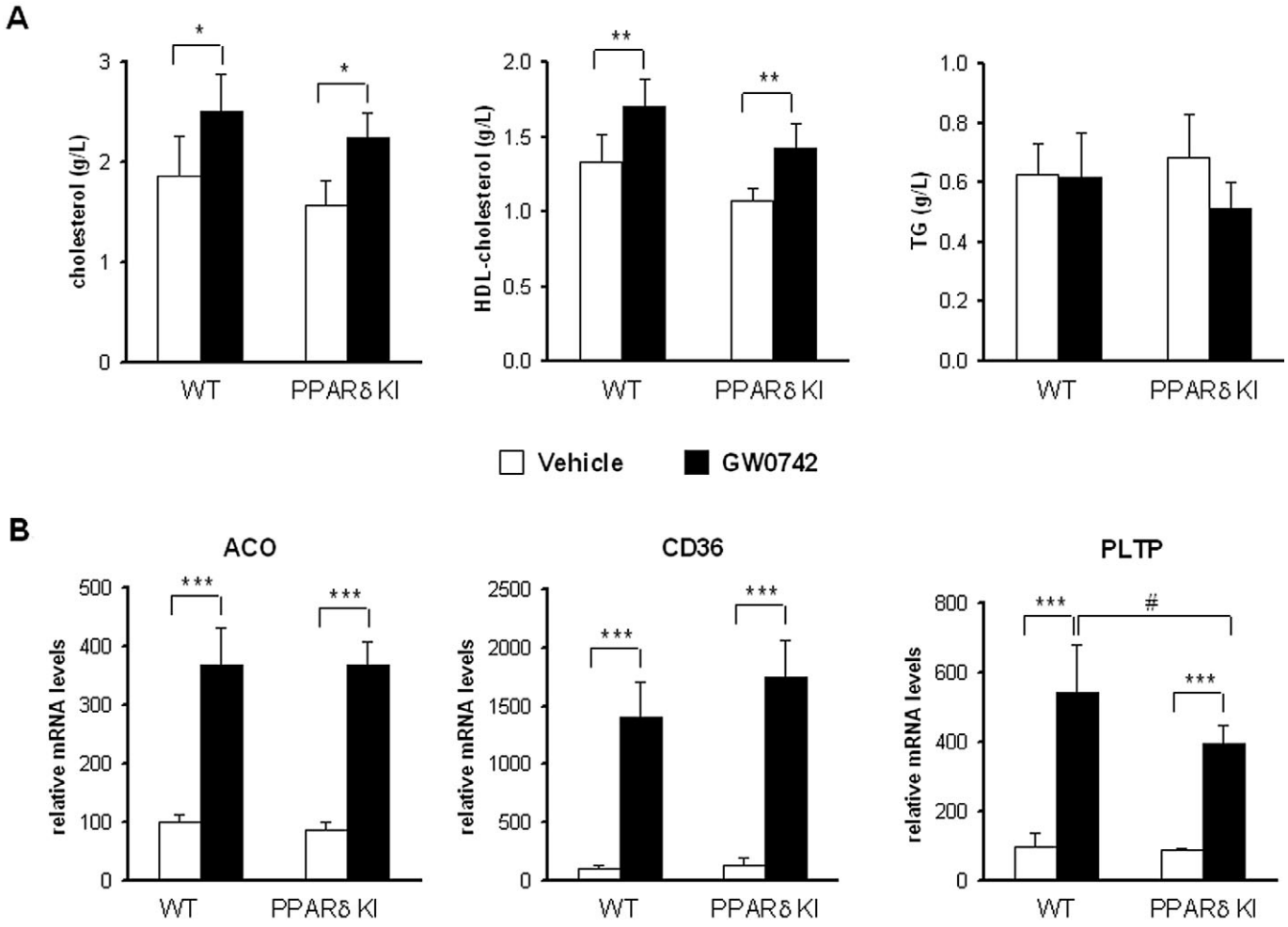

Figure 6

Similar response of hPPARδ KI and wild-type (WT) mice upon being fed a high-fat diet. (A) Plasma lipids were analysed in WT and PPARδ KI mice fed high-fat diet for 7 weeks followed by 14 days treatment with vehicle or GW0742 at 20 $mg \cdot kg^{-1} \cdot day^{-1}$. (B, C) Hepatic expression of genes involved in lipid metabolism and in the inflammatory response were analysed in vehicle- and GW0742-treated WT and PPARδ KI mice by quantitative PCR. Expression values are normalized to 36B4 and expression of vehicle-treated WT mice was set at 100. Values represent means ± SD. Significant differences by one-way ANOVA analysis. *$P < 0.05$; **$P < 0.005$; ***$P < 0.001$ vehicle versus GW0742. #$P < 0.05$; ##$P < 0.005$ ###$P < 0.001$ WT versus PPARδ KI. KI, knock-in.

differences in expression levels of nuclear receptor coactivators. The development of humanized mice for PPARδ allows us to establish the contribution of PPARδ protein sequence variations to the differential regulation observed between mouse and humans. This model is also useful to study the *in vivo* role of human PPARδ signalling pathways.

In our PPARδ KI mouse model, human PPARδ expression is under control of the native PPARδ mouse promoter. RT-PCR analysis with species-specific primers demonstrated the successful replacement of mouse PPARδ by its human orthologue. Furthermore, Northern blot analysis revealed that a full length mRNA was generated from the chimeric human PPARδ gene. Quantification of transcript levels indicated that human PPARδ mRNA levels are lower in some tissues, such as liver, small intestine, heart and macrophages, whereas its expression is similar in WAT, soleus and quadriceps muscles and skin. The presence of the neomycin expression cassette inserted in intron sequences has been reported to interfere with mRNA splicing, leading to a decreased expression level of the targeted gene (Nagy, 2000). This hypomorphic phenotype could be reversed upon removal of the neomycin expression cassette (Raffaï and Weisgraber, 2002). In our PPARδ KI model, the neomycin expression cassette introduced in the targeting vector is flanked by two LoxP sites allowing excision by the Cre recombinase. Breeding of PPARδ KI mice with MeuCre transgenic mice, which express the Cre recombinase ubiquitously at an early stage of embryo development (Leneuve *et al.*, 2003), indicated that excision of the neomycin expression cassette did not restore nor modify mRNA expression levels of the chimeric human PPARδ gene (data not shown). Therefore, the replacement of six exons and five introns by the cDNA sequence of human PPARδ probably eliminates regulatory sequences located in the removed introns. The existence of such regulatory

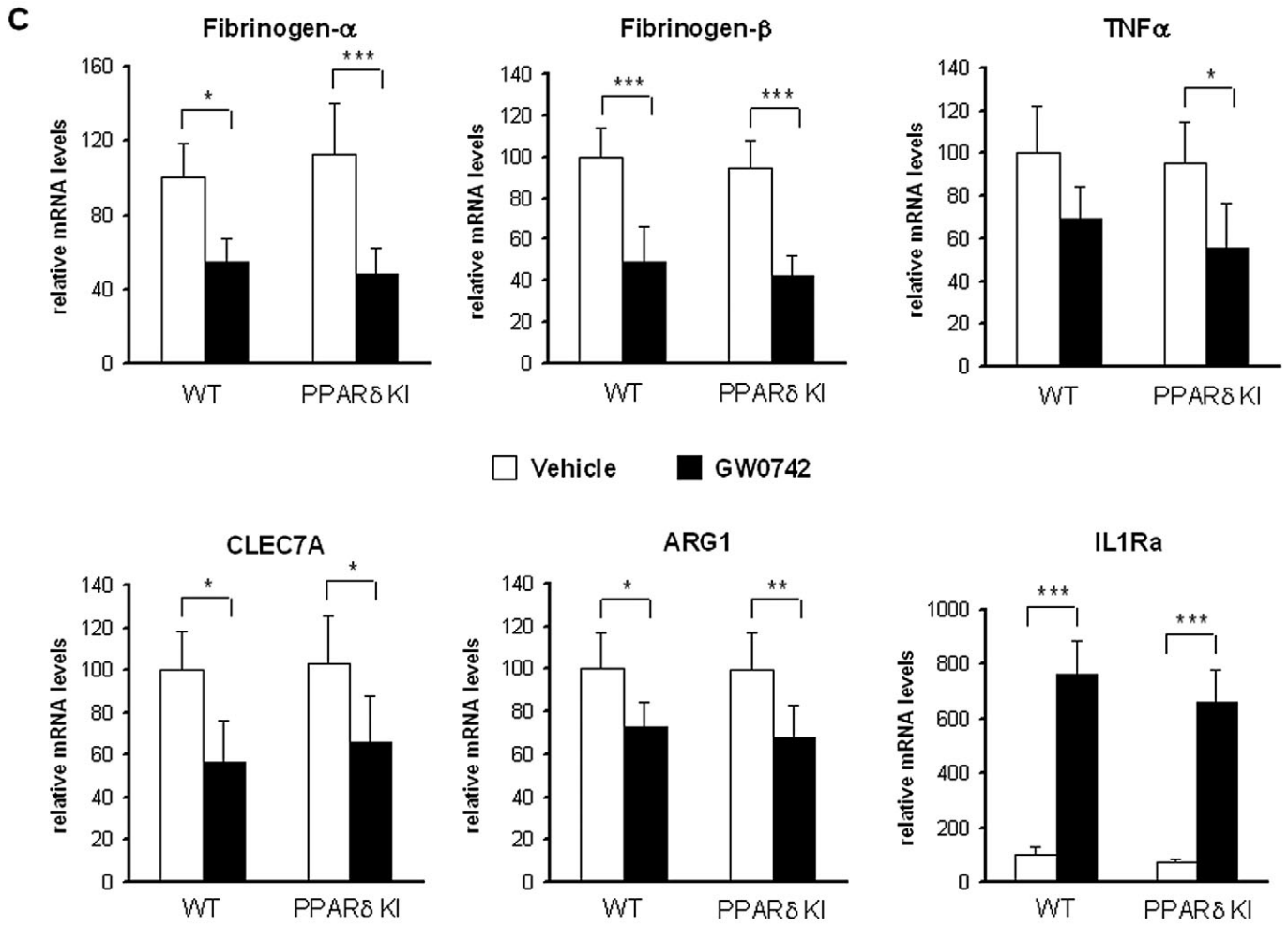

Figure 6
Continued.

elements were unknown at the time of the generation of the mouse model.

Replacement of mouse PPARδ by its human orthologue clearly leads to a functional protein, as PPARδ-deficiency generated embryonic lethality at the homozygous stage, which was not encountered in the PPARδ KI mouse model (Peters *et al.*, 2000; Barak *et al.*, 2002). The physiological effect of the replacement was first assessed in 10-week-old male and female mice. In male mice, expression of hPPARδ triggered a decrease of total cholesterol, mainly caused by the reduction of HDL-C. A reduction of LDL-C was also observed but this did not reach statistical significance. These effects could be due to the decreased level of PPARδ in some tissues. This down-regulation is associated, in liver and small intestine, with a reduction in PPARγ mRNA levels, and in macrophages with a decrease in PPARα mRNA levels, albeit the latter was not statistically significant. PPARγ was described to play a role in the modulation of the inflammatory response and fibrosis in liver (Kallwitz *et al.*, 2008) and small intestine (Wahli, 2008). It is unlikely that these compensatory changes in expression of PPARγ and PPARα explain this phenotype, although this cannot be formally excluded. Furthermore, the replacement and the decrease of PPARδ mRNA levels did not impact on TG metabolism as plasma TG did not change, supporting the conclusion that human PPARδ can fully replace mouse PPARδ activity in this pathway. Analysis of mRNA levels of genes involved in HDL and LDL homeostasis in liver did not identify differentially regulated genes, which would explain the decrease in HDL-C and LDL-C in the PPARδ KI mouse model.

Fasting is a physiological situation resulting in the activation of PPARδ by endogenous fatty acids released from adipose tissue (Sanderson *et al.*, 2009). Analysis of the metabolic response to fasting in PPARδ null mice indicated a role for PPARδ in the regulation of hepatic glucose and lipid metabolism, although the effects (reduced plasma cholesterol and increased glucose) are less marked compared with PPARα null mice (Sanderson *et al.*, 2010). PPARδ KI mice displayed a similar fasting response as WT mice. This was confirmed by similar changes in liver LPIN2 and ST3GAL5 mRNA levels in WT and PPARδ KI mice, the regulation of which has been reported to be PPARδ-dependent (Sanderson *et al.*, 2009; 2010).

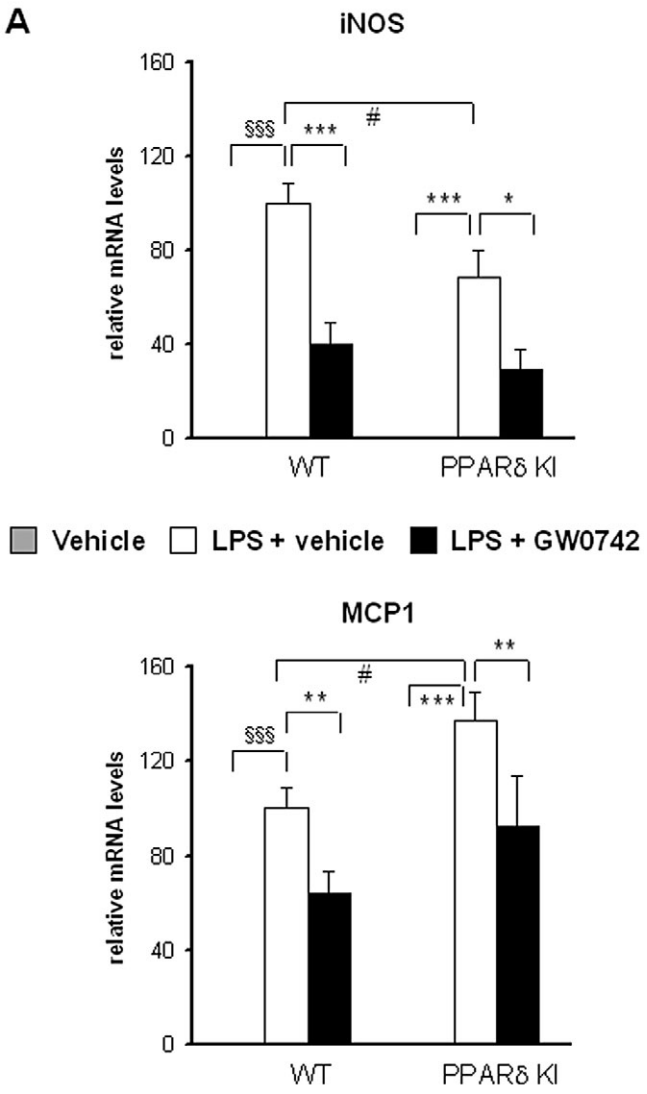

Figure 7

Effect of GW0742 treatment on gene regulation in peritoneal macrophages of wild-type (WT) and PPARδ KI mice. (A) Expression of genes involved in the inflammatory response was analysed by quantitative PCR in peritoneal macrophages from WT and PPARδ KI mice. Macrophages were treated with vehicle or LPS (100 ng·mL^{-1}) for 24 h in presence of vehicle or GW0742 (100 nM). Expression values are normalized to cyclophilin and expression of LPS + vehicle-treated WT macrophages was set at 100. Values represent means ± SD. Significant differences by one-way ANOVA analysis. §§§P < 0.005 vehicle versus LPS + vehicle; *P < 0.05; **P < 0.005; ***P < 0.001 LPS + vehicle versus LPS + GW0742. #P < 0.05 WT versus PPARδ KI. (B) Expression of genes involved in lipid homeostasis were analysed by quantitative PCR in peritoneal macrophages from WT and PPARδ KI mice treated with vehicle or GW0742 (100 nM) for 24 h. Expression values are normalized to cyclophilin and expression of vehicle-treated WT mice was set at 100. Values represent means ± SD. Significant differences by one-way ANOVA analysis. *P < 0.05; **P < 0.005; ***P < 0.001 vehicle versus GW0742. #P < 0.05; ##P < 0.005 ###P < 0.001 WT versus PPARδ KI. KI, knock-in.

The response of human PPARδ to activation was also assessed using a pharmacological approach with the GW0742 compound, a PPARδ–selective activator (Sznaidman *et al.*, 2003). The GW0742 compound is equipotent on human and mouse PPARδ as evaluated in cell-based transfection assay (EC_{50} ~30 nM for human PPARδ and EC_{50} ~50 nM for mouse PPARδ), with more than 1000-fold selectivity over mouse PPARα and mouse PPARγ (Graham *et al.*, 2005). Consistent with the role of PPARδ activation in improving the blood lipid profile in humans and in different animal models (Leibowitz *et al.*, 2000; Oliver *et al.*, 2001; van der Veen *et al.*, 2005; Wallace *et al.*, 2005; Sprecher *et al.*, 2007; Risérus *et al.*, 2008; Roberts *et al.*, 2009), GW0742 treatment induced HDL-C to a similar extent in both strains of mice. GW0742 treatment had also a minor effect on TG levels with a decreased TG content in LDL particles in both WT and PPARδ KI mice. By contrast, GW0742 treatment induced an increase in LDL-C, in line with recent results of Briand *et al.* (Briand *et al.*, 2009) obtained with GW0742 in mice with a similar genetic background to those in our study. Overall, activation of human PPARδ triggered similar biological effects in mice fed a normal chow diet and HFD fed mice. Moreover, activation of hPPARδ resulted in a similar anti-inflammatory response in liver and macrophages of WT and PPARδ KI mice.

Consistent with the biological effects, analysis of transcription levels of a number of genes involved in lipoprotein and lipid metabolism in liver, soleus muscle and macrophages showed similar patterns of regulation in both mouse models. Interestingly, despite a lower level of expression of PPARδ in the liver and macrophages, few differences in the amplitude of gene regulation could be detected suggesting that 50% of transcript levels of PPARδ is sufficient to maintain an optimal response by the PPARδ activator. Although *in vivo* studies showed a plasma concentration of GW0742 of 1 μM at a dose of 20 mg·kg^{-1}·day^{-1} in mice (van der Veen *et al.*, 2005), we cannot exclude the possibility that higher concentrations of GW0742 are achieved in tissues such as the liver, which could result in the activation of other PPARs. However, it is noteworthy that transcript levels of several classical PPARα-regulated genes, such as APOA1, APOA2 and CPT1a, were not modified in livers of GW0742-treated mice, rendering this possibility unlikely, although a partial activation of PPARα, with regulation of only a subset of PPARα target genes, by GW0742 cannot be formally excluded.

The PPARδ KI mouse model was also used to investigate the human–mouse dissimilarities in PPARδ regulation of genes involved in cholesterol and lipid trafficking in macrophages such as ABCA1, LXRα and A-FABP. In contrast to PPARδ-induced regulation in human macrophages (Vosper *et al.*, 2001; Lee *et al.*, 2003; Li *et al.*, 2004), mRNA levels of ABCA1, LXRα and A-FABP were not changed upon GW0742 treatment in macrophages from WT and PPARδ KI mice. Despite decreased hPPARδ transcript levels, hPPARδ activation resulted in regulation of ACO, CPT1a, MCP1 and iNOS. A similar functional response to hPPARδ activation was also observed *in vivo* in Kupffer cells. Therefore the lack of responsiveness of macrophages to GW0742 for ABCA1, LXRα and A-FABP in PPARδ KI, as in WT, is not caused by differences in the PPARδ protein sequence between mouse and human. Distinct methodologies used for the isolation of human and mouse macrophages, differentiated blood monocytes for

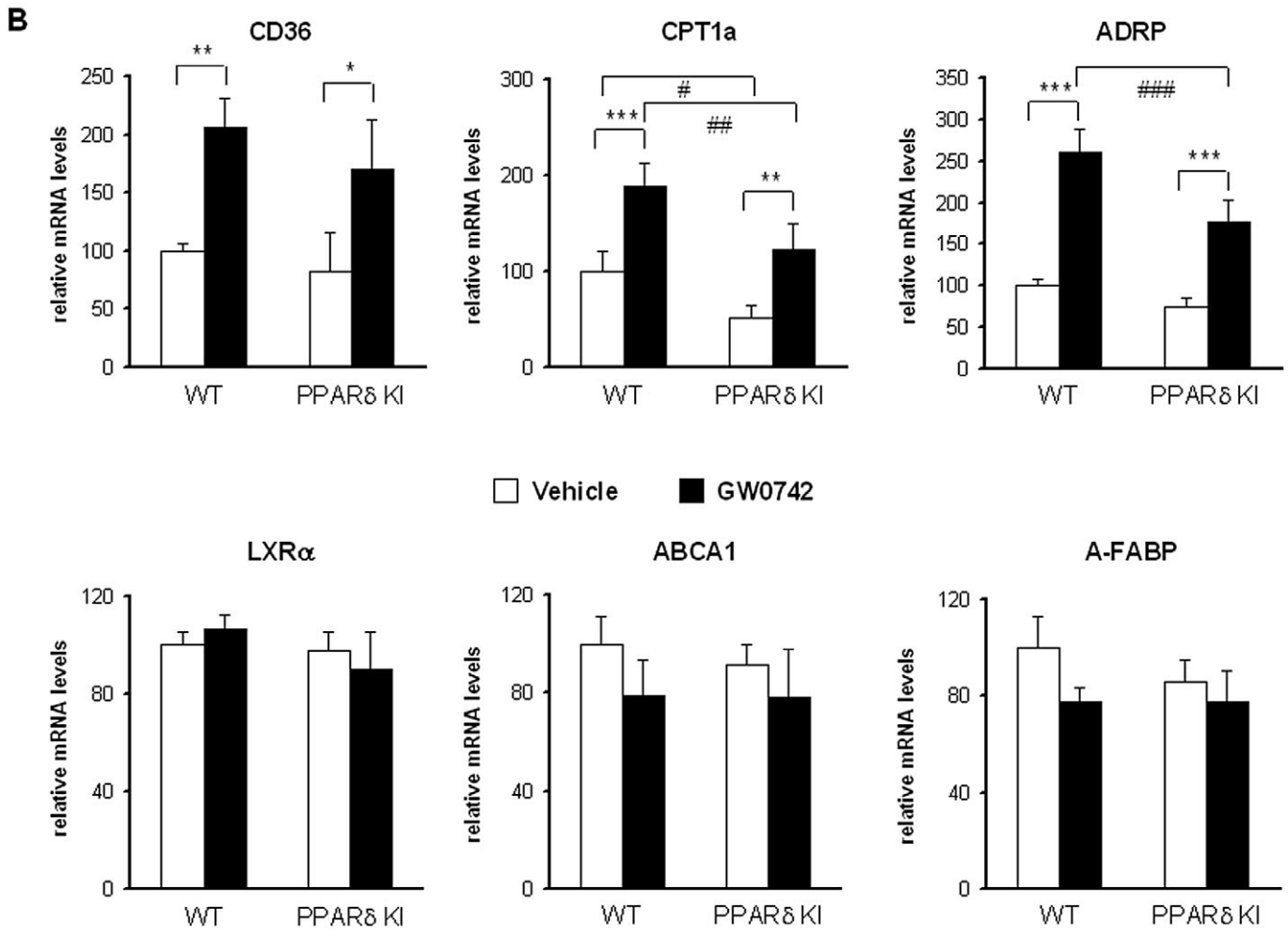

Figure 7
Continued.

human macrophages versus peritoneal or bone marrow derived macrophages for mouse, could explain the differential regulation of these genes between mouse and human macrophages.

In conclusion, our humanized mouse model for PPARδ shows that human PPARδ is able to replace the function of mouse PPARδ. Using the PPARδ-specific activator, GW0742, we have shown that mouse and human PPARδ have similar functions in lipid and lipoprotein metabolism as a consequence of the regulation of a similar gene repertoire. Therefore, this study underscores the use of this PPARδ KI mouse model for the study of the function of human PPARδ and as a tool for preclinical assessment of novel PPARδ activators with a human spectrum of action.

Acknowledgements

We are grateful to E. Teissier (Inserm, U1011) for technical help and V. Beneton (GlaxoSmithKline, Les Ulis, France) for providing the GW0742 compound. This work was supported by grants from Leducq Foundation and Conseil Régional Nord-Pas de Calais.

Conflict of interest

D. Grillot is employed by GlaxoSmithKline, F-91951, Les Ulis, France. B. Gross, N. Hennuyer, E. Bouchaert, C. Rommens, H. Mezdour and B. Staels state no conflict of interest.

References

Barak Y, Liao D, He W, Ong ES, Nelson MC, Olefsky JM *et al.* (2002). Effects of peroxisome proliferator-activated receptor δ on placentation, adiposity, and colorectal cancer. Proc Natl Acad Sci USA 99: 303–308.

Barish GD, Narkar VA, Evans RM (2006). PPARδ: a dagger in the heart of the metabolic syndrome. J Clin Invest 116: 590–597.

Briand F, Naik SU, Fuki I, Millar JS, Macphee C, Walker M *et al.* (2009). Both the peroxisome proliferator-activated receptor (PPAR) delta agonist, GW0742, and ezetimibe promote reverse cholesterol transport in mice by reducing intestinal re-absorption of HDL-derived cholesterol. Clin Transl Sci 2: 127–133.

Bugge A, Grøntved L, Aagaard MM, Borup R, Mandrup S (2009). The PPARgamma2 A/B-domain plays a gene-specific role in transactivation and cofactor recruitment. Mol Endocrinol 23: 794–808.

Chawla A, Lee CH, Barak Y, He W, Rosenfeld J, Liao D *et al.* (2003). PPARδ is a very low-density lipoprotein sensor in macrophages. Proc Natl Acad Sci USA 100: 1268–1273.

Dressel U, Allen TL, Pippal JB, Rohde PR, Lau P, Muscat GE (2003). The peroxisome proliferator-activated receptor β/δ agonist, GW501516, regulates the expression of genes involved in lipid catabolism and energy uncoupling in skeletal muscle cells. Mol Endocrinol 17: 2477–2493.

Ehrenborg E, Krook A (2009). Regulation of skeletal muscle physiology and metabolism by peroxisome proliferator-activated receptor δ. Pharmacol Rev 61: 373–393.

Escher P, Braissant O, Basu-Modak S, Michalik L, Wahli W, Desvergne B (2001). Rat PPARs: quantitative analysis in adult rat tissues and regulation in fasting and refeeding. Endocrinology 142: 4195–4202.

Girroir EE, Hollingshead HE, He P, Zhu B, Perdew GH, Peters JM (2008). Quantitative expression patterns of peroxisome proliferator-activated receptor-β/δ (PPARβ/δ) protein in mice. Biochem Biophys Res Commun 371: 456–461.

Gonzalez FJ, Shah YM (2008). PPARα: mechanism of species differences and hepatocarcinogensis of peroxisome proliferators. Toxicology 246: 2–8.

Graham TL, Mookherjee C, Suckling KE, Palmer CN, Patel L (2005). The PPARδ agonist GW0742X reduces atherosclerosis in LDLR-/- mice. Atherosclerosis 181: 29–37.

Gross B, Staels B (2007). PPAR agonists: multimodal drugs for the treatment of type-2 diabetes. Best Pract Res Clin Endocrinol Metab 21: 687–710.

Gross BS, Fruchart JC, Staels B (2005). Peroxisome proliferator-activated receptor β/δ: a novel target for the reduction of atherosclerosis. Drug Discov Today 2: 237–243.

Higashiyama H, Billin AN, Okamoto Y, Kinoshita M, Asano S (2007). Expression profiling of peroxisome proliferator-activated receptor-δ (PPAR-δ) in mouse tissues using tissue microarray. Histochem Cell Biol 127: 485–494.

Huang W, Zhang J, Wei P, Schrader WT, Moore DD (2004). Meclizine is an agonist ligand for mouse constitutive androstane receptor (CAR) and an inverse agonist for human CAR. Mol Endocrinol 18: 2402–2408.

Hummasti S, Tontonoz P (2006). The peroxisome proliferator-activated receptor N-terminal domain controls isotype-selective gene expression and adipogenesis. Mol Endocrinol 20: 1261–1275.

Kallwitz ER, McLachlan A, Cotler SJ (2008). Role of peroxisome proliferators-activated receptors in the pathogenesis and treatment of nonalcoholic fatty liver disease. World J Gastroenterol 14: 22–28.

Keller H, Devchand PR, Perroud M, Wahli W (1997). PPARα structure-function relationship derived from species-specific differences in responsiveness to hypolipidemic agents. Biol Chem 378: 651–655.

Lalloyer F, Pedersen TA, Gross B, Lestavel S, Yous S, Vallez E *et al.* (2009). Rexinoid bexarotene modulates triglyceride but not cholesterol metabolism via gene-specific permissivity of the RXR/LXR heterodimer in the liver. Arterioscler Thromb Vasc Biol 29: 1488–1495.

Lee SS, Pineau T, Drago J, Lee EJ, Owens JW, Kroetz DL *et al.* (1995). Targeted disruption of the α isoform of the peroxisome proliferator-activated receptor gene on mice results in abolishment of the pleiotropic effects of peroxisome proliferators. Mol Cell Biol 15: 3012–3022.

Lee CH, Chawla A, Urbiztondo N, Liao D, Boisvert WA, Evans RM *et al.* (2003). Transcriptional repression of atherogenic inflammation: modulation by PPARδ. Science 302: 453–457.

Lee CH, Kang K, Mehl IR, Nofsinger R, Alaynick WA, Chong L *et al.* (2006). Peroxisome proliferator-activated receptor δ promotes very low-density lipoprotein-derived fatty acid catabolism in the macrophage. Proc Natl Acad Sci USA 103: 2434–2439.

Lefebvre P, Chinetti G, Fruchart JC, Staesl B (2006). Sorting out the roles of PPARα in energy metabolism and vascular homeostasis. J Clin Invest 116: 571–580.

Leibowitz MD, Fiévet C, Hennuyer N, Peinado-Onsurbe J, Duez H, Bergera J *et al.* (2000). Activation of PPARδ alter lipid metabolism in db/db mice. FEBS Lett 473: 333–336.

Leneuve P, Colnot S, Hamard G, Francis F, Niwa-Kawakita M, Giovannini M *et al.* (2003). Cre-mediated germline mosaicism: a new transgenic mouse for the selective removal of residual markers from tri-lox conditional alleles. Nucleic Acid Res 31: e21.

Li AC, Binder CJ, Gutierrez A, Brown KK, Plotkin CR, Pattison JW *et al.* (2004). Differential inhibition of macrophage foam-cell formation and atherosclerosis in mice by PPARα, β/δ, and γ. J Clin Invest 114: 1564–1576.

Luo J, Quan J, Tsai J, Hobensack CK, Sullivan C, Hector R *et al.* (1998). Nongenetic mouse models of non-insulin-dependent diabetes mellitus. Metabolism 47: 663–668.

Morimura K, Cheung C, Ward JM, Reddy JK, Gonzalez FJ (2006). Differential susceptibility of mice humanized for peroxisome proliferator-activated receptor α to Wy-14,643-induced liver tumorigenesis. Carcinogenesis 27: 1074–1080.

Muoio DM, MacLean PS, Lang DB, Li S, Houmard JA, Way JM *et al.* (2002). Fatty acid homeostasis and induction of lipid regulatory genes in skeletal muscles of peroxisome proliferator-activated receptor (PPAR) α knock-out mice. J Chem Biol 277: 26089–26097.

Nagy A (2000). Cre recombinase: the universal reagent for genome tailoring. Genesis 26: 99–109.

Odegaard JI, Ricardo-Gonzalez RR, Eagle AR, Vats D, Morel CR, Goforth MH *et al.* (2008). Alternative M2 activation of Kupffer cells by PPARδ ameliorates obesity-induced insulin resistance. Cell Metabolism 7: 496–507.

Oliver WR Jr, Shenk JL, Snaith MR, Russell CS, Plunket KD, Bobkin NL *et al.* (2001). A selective peroxisome proliferator-activated receptor δ agonist promotes reverse cholesterol transport. Proc Natl Acad Sci USA 98: 5306–5311.

Peters JM, Lee SS, Li W, Ward JM, Gavrilova O, Everett C *et al.* (2000). Growth, adipose, brain, and skin alteration resulting from targeted disruption of the mouse peroxisome proliferator-activated receptor β(δ). Mol Cell Biol 20: 5119–5128.

Raffaï RL, Weisgraber KH (2002). Hypomorphic apolipoprotein E mice: a new model of conditional gene repair to examine apolipoprotein E-mediated metabolism. J Biol Chem 277: 11064–11068.

Ram VJ (2003). Therapeutic role of peroxisome proliferator-activated receptors in obesity, diabetes and inflammation. Prog Drug Res 60: 96–132.

Risérus U, Sprecher D, Johnson T, Olson E, Hirschberg S, Liu A *et al.* (2008). Activation of PPARδ promotes reversal of multiple metabolic abnormalities, reduces oxidative stress and increases fatty acid oxidation in moderately obese man. Diabetes 57: 332–339.

Roberts LD, Hassall DG, Winegar DA, Haselden JN, Nicholls AW, Griffin JL (2009). Increased hepatic oxidative metabolism distinguishes the action of peroxisome proliferator-activated receptor δ from peroxisome proliferator-activated receptor γ in the *ob/ob* mouse. Genome Med 1: 115.

Sanderson LM, Degenhardt T, Koppen A, Kalkhoven E, Desvergne B, Müller M *et al.* (2009). Peroxisome proliferator-activated receptor β/δ but not PPARα serves as a plasma free fatty acid sensor in liver. Mol Cell Biol 29: 6257–6267.

Sanderson LM, Boekschoten MV, Desvergne B, Müller M, Kersten S (2010). Transcriptional profiling reveals divergent roles of PPARα and PPARβ/δ in regulation of gene expression in mouse liver. Physiol Genomics 41: 42–52.

Sprecher DL, Massien C, Pearce G, Billin AN, Perlstein I, Willson TM *et al.* (2007). Triglyceride: High-density lipoprotein cholesterol effects in healthy subjects administered a peroxisome proliferator activated receptor δ agonist. Arterioscler Thromb Vasc Biol 27: 359–365.

Sznaidman ML, Haffner CD, Maloney PR, Fivush A, Chao E, Goreham D *et al.* (2003). Novel selective small molecule agonists for peroxisome proliferator-activated receptor δ (PPARδ)-synthesis and biogical activity. Bioorg Med Chem Lett 13: 1517–1521.

Tanaka T, Yamamoto J, Iwasaki S, Asaba H, Hamura H, Ikeda Y *et al.* (2003). Activation of peroxisome proliferator-activated receptor δ induces fatty acid β-oxidation in skeletal muscle and attenuates metabolic syndrome. Proc Natl Acad Sci USA 100: 15924–15929.

van der Veen JN, Kruit JK, Havinga R, Baller JF, Chimini G, Lestavel S *et al.* (2005). Reduced cholesterol absorption upon PPARδ activation coincides with decreased intestinal expression of NPC1L1. J Lipid Res 46: 526–534.

Vosper H, Patel L, Graham TL, Khoudoli GA, Hill A, Macphee CH *et al.* (2001). The peroxisome proliferator-activated receptor δ promotes lipid accumulation in human macrophages. J Biol Chem 276: 44258–44265.

Wahli W (2008). A gut feeling of the PXR, PPAR and NF-κB connection. J Intern Med 263: 613–619.

Wallace JM, Schwarz M, Coward P, Houze J, Sawyer JK, Kelley KL *et al.* (2005). Effects of peroxisome proliferator-activated receptor α/δ agonists on HDL-cholesterol in vervet monkeys. J Lip Res 46: 1009–1016.

Wang YX, Zhang CL, Yu RT, Cho HK, Nelson MC, Bayuga-Ocampo CR *et al.* (2004). Regulation of muscle fiber type and running endurance by PPARδ. Plos Biol 2: e294.

Welch JS, Ricote M, Akiyama TE, Gonzalez FJ, Glass CK (2003). PPARγ and PPARδ negatively regulate specific subsets of lipopolysaccharide and IFN-γ target genes in macrophages. Proc Natl Acad Sci USA 100: 6712–6717.

Xie W, Barwick JL, Downes M, Blumberg B, Simon CM, Nelson MC *et al.* (2000). Humanized xenobiotic response in mice expressing nuclear receptor SXR. Nature 406: 435–439.

Supporting information

Additional Supporting Information may be found in the online version of this article:

Figure S1 The size of PPARδ mRNA of WT and PPARδ KI mice is similar. mRNA isolated from liver, small intestine, white adipose tissue, and skin of WT (+/+), PPARδ KI heterozygote (+/KI) and homozygote (KI/KI) mice was analysed by Northern blot using a probe located in the 3′UTR of mouse *PPARδ*.
Figure S2 FPLC separation of plasma lipoproteins of 10-week-old male WT and PPARδ KI mice fed a chow diet. Plasma from individual WT (open squares) and PPARδ KI (black circles) mice was separated by gel filtration coupled to an online cholesterol (A) and triglyceride (B) determination system. Data are a mean representation of 22 and 28 animals for WT and PPARδ KI mice respectively.
Figure S3 FPLC separation of plasma lipoproteins of GW0742-treated WT and PPARδ KI male mice. WT and PPARδ KI mice were gavaged with vehicle or GW0742 (20 $mg \cdot kg^{-1} \cdot day^{-1}$) for 14 days. Plasma from individual mice were separated by gel filtration coupled to an online cholesterol (A) and triglyceride (B) determination system. Data are a mean representation of eight mice per group.
Figure S4 Response of PPARδ KI mice to a high-fat diet. (A) WT and PPARδ KI mice were fed (n = 12–14 per group) during 7 weeks a high-fat diet (HFD) containing 35.5% of fat. Weight gain of WT (open squares) and PPARδ KI (black circles) mice is expressed in percentage of body weight at day 0. (B) After 7 weeks of HFD, mice were treated with vehicle (white bars) or GW0742 (20 $mg \cdot kg^{-1} \cdot day^{-1}$, black bars) for 14 days (n = 6–8 per group). Body weight, blood glucose, insulin levels and liver weight were measured.

Please note: Wiley-Blackwell are not responsible for the content or functionality of any supporting materials supplied by the authors. Any queries (other than missing material) should be directed to the corresponding author for the article.